

# Supporting Information

## Self-assembly of CTAB surfactant on gold nanoparticle: An united-atom molecular dynamics simulation study

Pandurangan Kalipillai <sup>a</sup>, E. Raghuram<sup>a</sup>, Sulalit Bandyopadhyay<sup>b</sup>, and Ethayaraja Mani <sup>a\*</sup>

<sup>a</sup> *Polymer Engineering and Colloid Science Lab, Department of Chemical Engineering, Indian Institute of Technology Madras, Chennai - 600036, India.*

<sup>b</sup> *Department of Chemical Engineering, Faculty of Natural Sciences, Norwegian University of Science and Technology, N – 7491 Trondheim, Norway.*

E-mail: ethaya@iitm.ac.in

## I. Minimum distance calculation

The schematic of minimum distance ( $D_{min}$ ) between CTAB tail end atom (C20) with AuNP surface is shown in Figure S1. The  $D_{min}$  for all the CTAB in all the three different system SP1, SP2 and SP3 are calculated. The  $D_{min}$  reveals, only the CTAB tail closely adsorb on the AuNP surface.

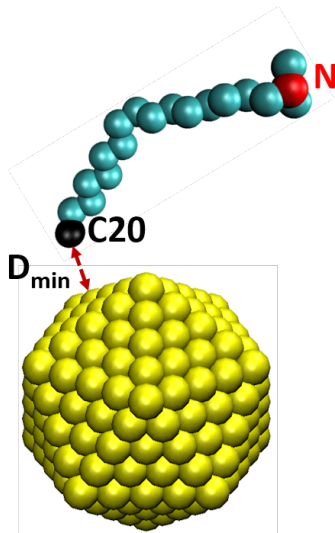


Figure S1: Schematic for  $D_{min}$  Au-C20.

The adsorption contact map is prepared and shown in Figures S2, S3 and S4 respectively for SP1, SP2 and SP3 for 100 ns with the cut-off distance 0.5 nm obtained from  $g(r)$  analysis of Au-C20 pair. The red circle indicates the free CTAB and the green filled circle indicates adsorbed CTAB on AuNP surface. The CTAB index (#) vs time,  $N_{ad}$  is calculated by adding green filled circle for last 50 ns.

## II. Effect of initial configuration

In order to confirm that the initial configuration does not affect the equilibrium configurations, we took two different random(IC1) vs regular(IC2) initial packing of CTAB around SP1 surface shown in Figures S5 (a) and (b). Here, for the clarity  $Br$  ions and the water molecules are not shown in the figure.

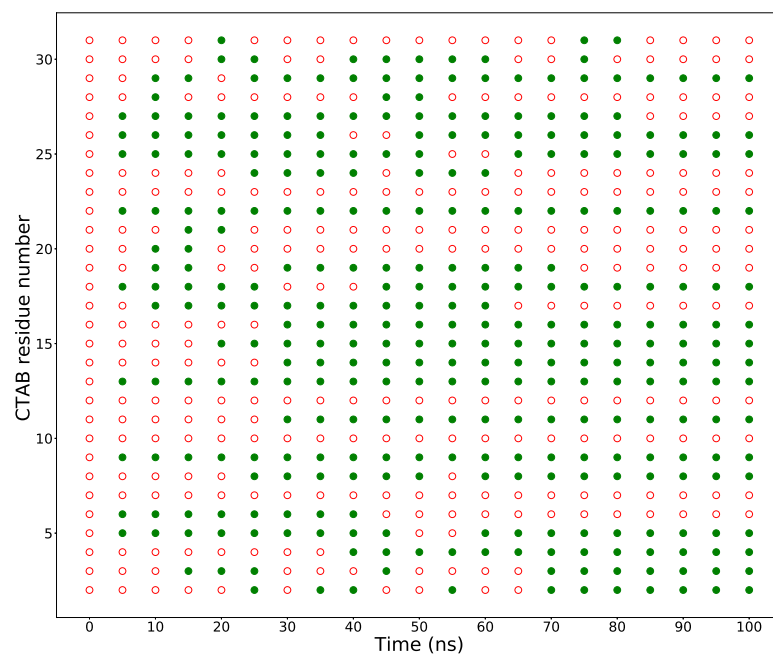


Figure S2: Adsorption dynamics between AuNP-CTAB SP1.

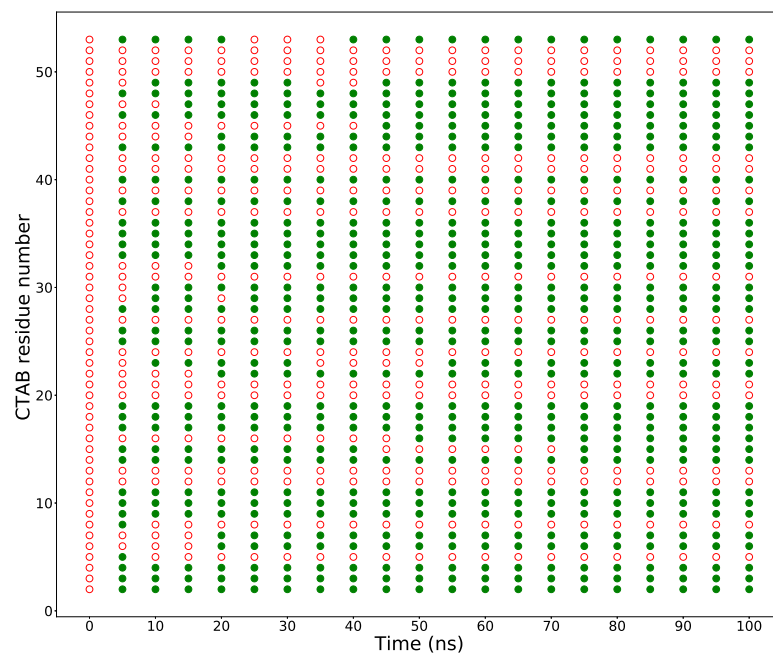


Figure S3: Adsorption dynamics between AuNP-CTAB SP2.

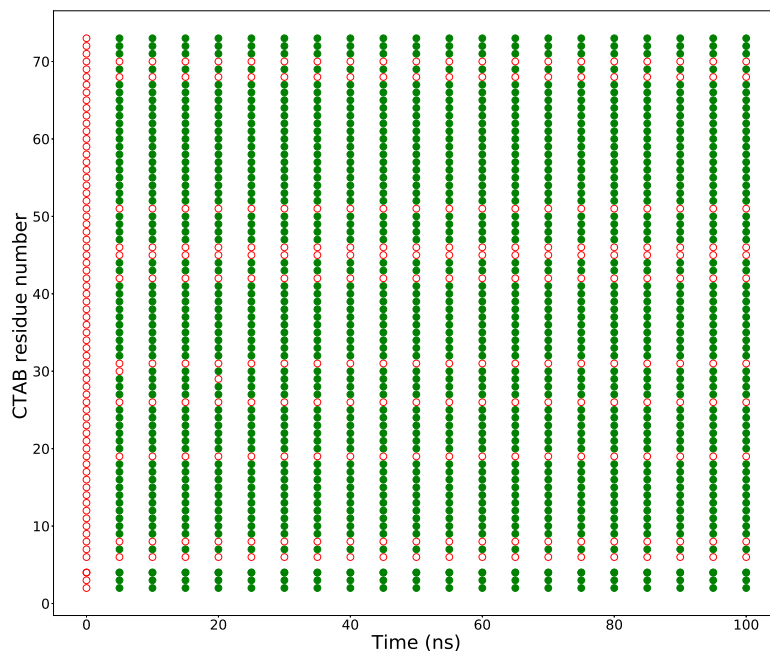


Figure S4: Adsorption dynamics between AuNP-CTAB SP3.

The minimum distance between C20-AuNP and N-AuNP for two different initial configuration IC1 and IC2 is shown in Figures S6 (a) and (b). It can be observed that, after 50 ns the distance between all the C20-AuNP and N-AuNP matches well for two different initial configuration IC1 and IC2. Therefore, irrespective initial configuration of CTAB around AuNP leads to the same type of CTAB self-assembly.

The pair distribution function  $g(r)$  for different atom pair for two initial configuration is shown Figures S7. Invariably  $g(r)$  Au-N in Figure (S7c), Au-C20 in Figure (S7a), Au-Br in Figure (S7d) and Au-O in Figure (S7b) absolutely matches well with both different initial configuration IC1 and IC2. Therefore, the monolayer self-assembly does not seem to depend on the initial configuration of the CTAB packing around AuNP. One more illustration for the effect of initial configuration discussed here. The IC2 (CTAB tail near AuNP) and IC3 (CTAB head near AuNP) is shown in Figures S8 (a) and (b). The distance between C20-



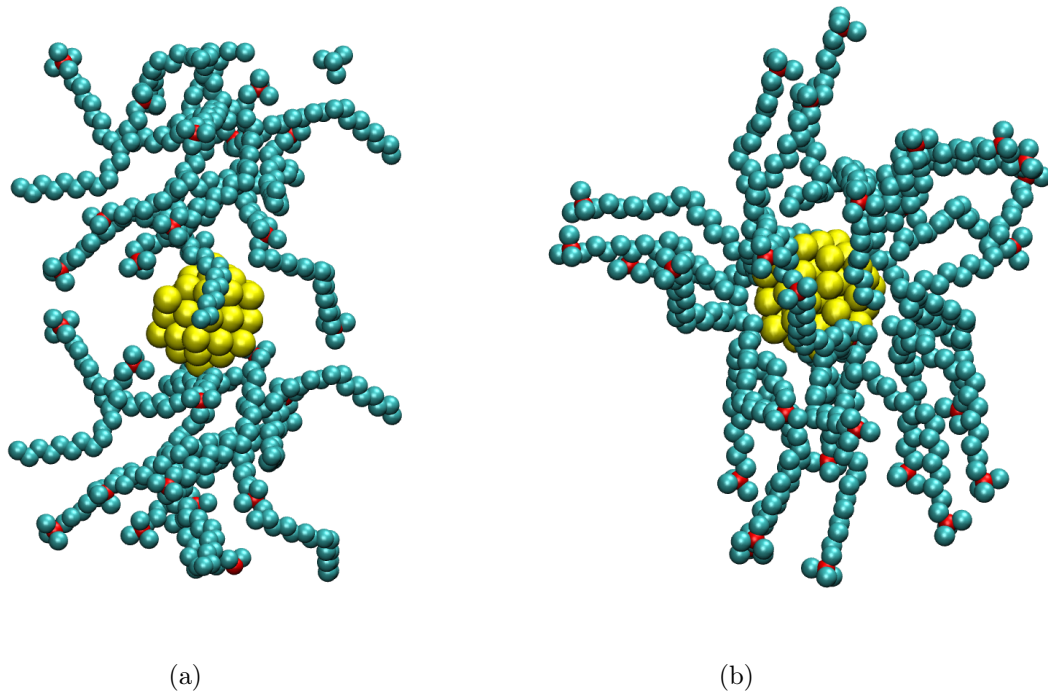


Figure S5: Initial configurations of SP1. (a) IC1 and (b) IC2. Au atom: yellow; CTAB: cyan and the head group N: blue.

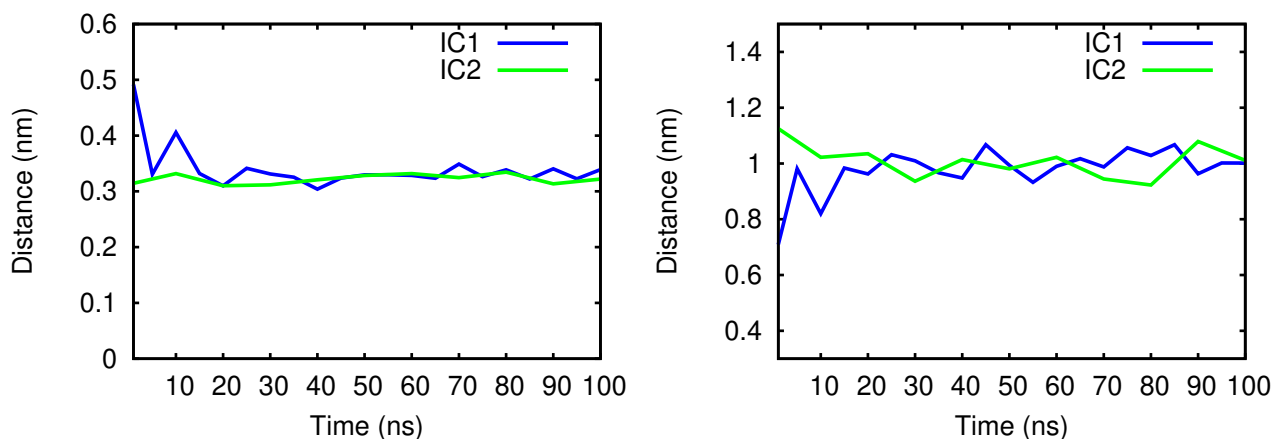


Figure S6: Comparison of distance between CTAB-AuNP for IC1 and IC2. (a) Au-C20 and (b) Au-N

AuNP for IC2 and IC3 is shown in Figures S9 (a) and (b). It can be observed that, after 25 ns the distance between all the C20-AuNP matches well for two different initial configuration IC2 and IC3. Therefore, irrespective initial configuration of CTAB around AuNP leads to the same type of CTAB self-assembly.

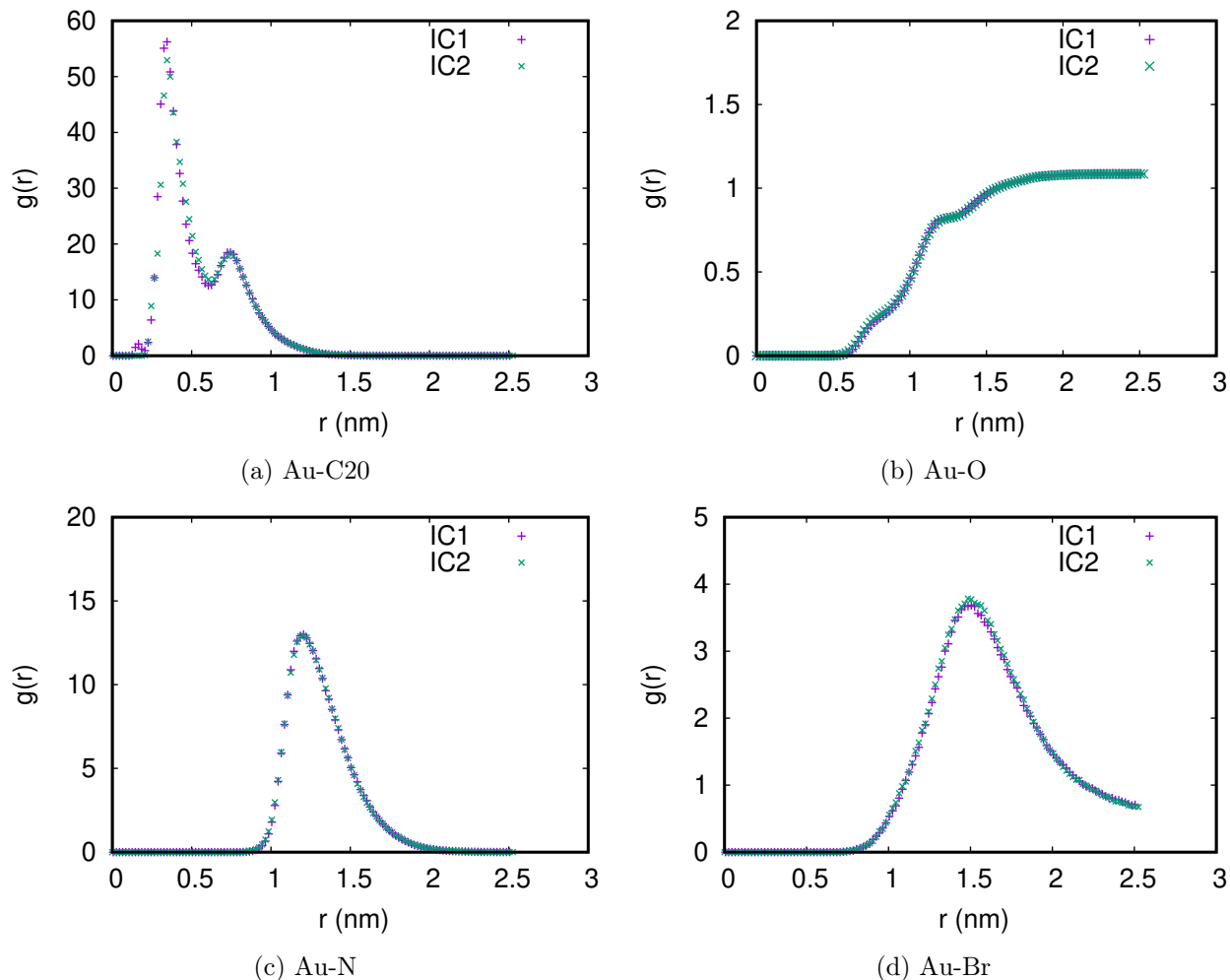


Figure S7: The pair distribution functions  $g(r)$  for specific atomic pairs (a) Au-C20, (b) Au-O, (c) Au-N and (d) Au-Br for two different initial configurations IC1 and IC2.

### III. Parameters used in binding free energy (BFE)

To assess the strength of adsorption, binding free energy between CTAB and gold nanoparticle is calculated using Molecular Mechanics - Poisson Boltzmann Solvent Area (MM-PBSA) method.<sup>1</sup> The parameters used in BFE calculation are listed in Table.S1.

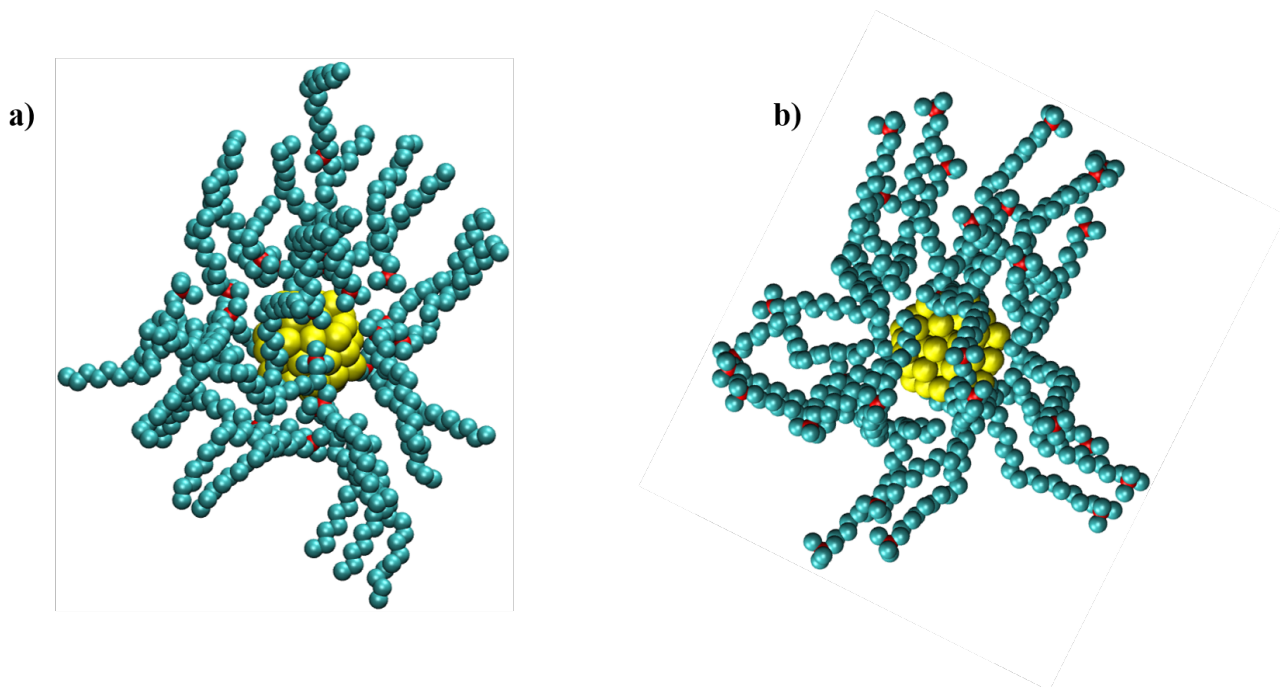


Figure S8: Initial configurations (a)IC3 (Head of CTAB around AuNP), (b) IC2 (Tail of CTAB around AuNP).

**Table S1: Parameters used in binding free energy calculation.<sup>1,2</sup>**

Parameters(P)	P notation in code	Values
Solute dielectric constant-CTAB	pdie	2.0
Solvent dielectric constant-Water	sdie	80
Vacuum dielectric constant	vdie	1.0
Surface tension(kJ/mol A <sup>2</sup> )	gamma	0.022678
Probe radius (A <sup>o</sup> )	sasrad	1.40
Offset constant (kJ/mol)	sasaconstant	3.84982
Temperature (K)	APtemp	300

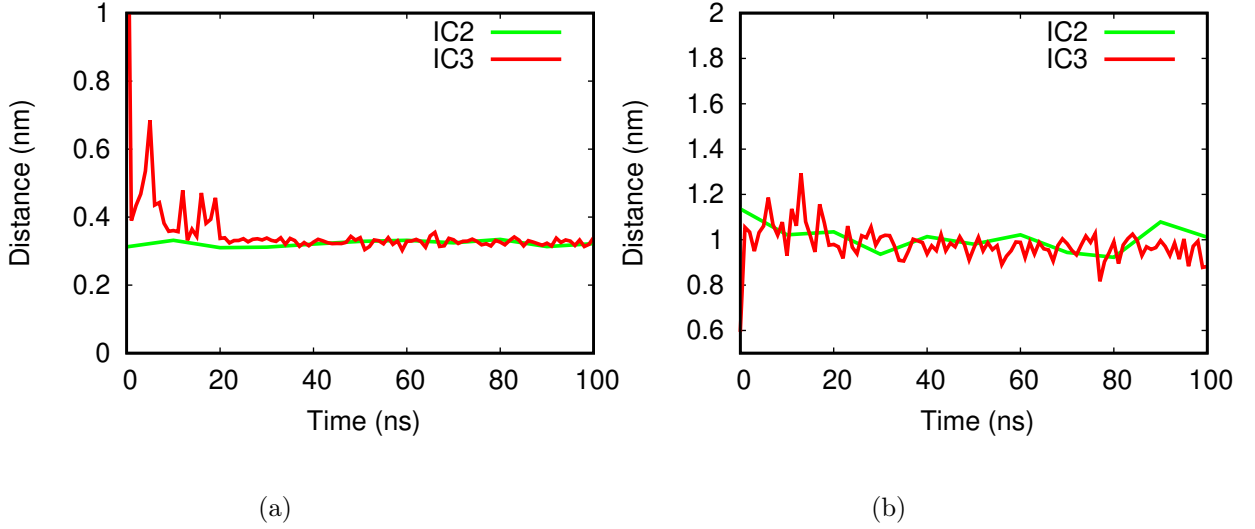


Figure S9: Comparison of distance between CTAB-AuNP for IC2 and IC3. (a) Au-C20 and (b) Au-N.

## IV. System size effect

To see the system size effect, we doubled number of surfactant molecules and counter-ions, and corresponding the number of water molecules are taken so as to maintain 250 CMC or 0.25 mol/lit the concentration of CTAB. Then, the new systems are termed as SP1\* and SP2\* as shown in Table S2.

**Table S2: Parameters used in the system size effect simulations**

	SP1	SP1*	SP2	SP2*
$N_s$	30	60	52	104
$N_{Br}$	30	60	52	104
$N_w$	3820	7640	10443	20886
$L_B$ (nm)	6.06	6.90	7.28	9.10

$N_s$ ,  $N_{Br}$ ,  $N_w$  are the number of CTAB,  $Br^-$  and water, respectively.  $L_B$  is initial length of simulation box.

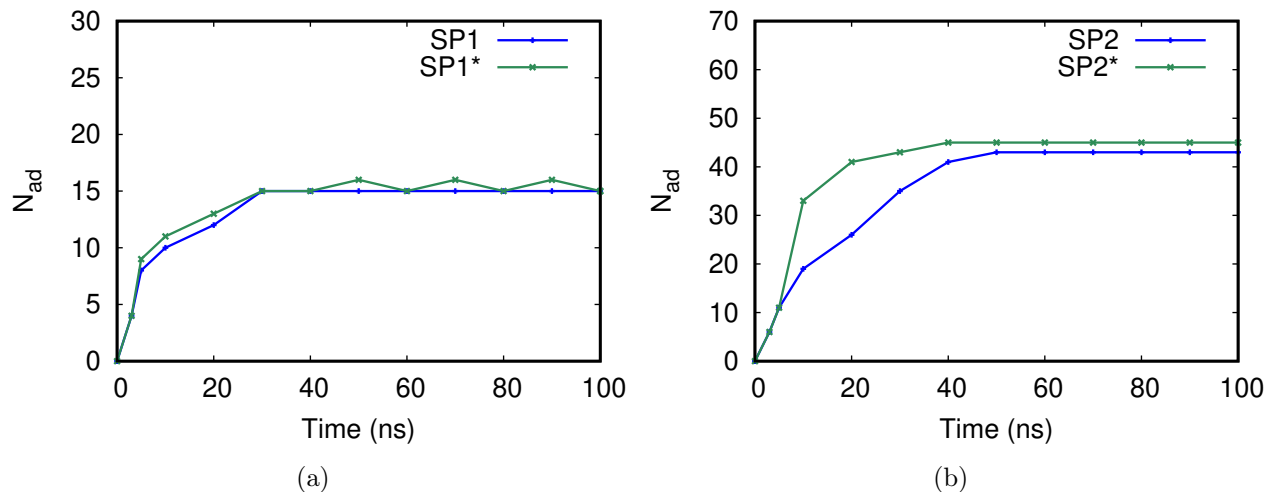


Figure S10: Number of adsorbed CTAB ( $N_{ad}$ ) on the AuNP surface with respect to time: (a) SP1 and (b) SP2.

We can observe from Fig.S10 (a) and (b) that the number of adsorbed CTAB molecules remains almost the same when system size is doubled for SP1 and SP2. Therefore monolayer adsorption of CTAB on AuNP surface is not limited by the number of CTAB surfactant molecules which we used in our simulations.

## V. Pre-formed bilayer on spherical gold nanoparticle

Here, we have taken four different initial configurations (r0, r1, r2 and r3) of SP2 with 95 Br immobilized on the surface and 2 CTAB as shown in Fig. S11. Where, r0 - tail-tail overlap of and head of one the CTAB overlap with Br ions and the overlaps are highlighted with circles. Basically r1, r2 and r3 are different configurations with increasing distance between CTAB tail ends (vertical black arrows) and CTAB's chain-chain distance (horizontal red arrows). Energy minimization done for these four configuration to understand favourable Starting structure to a build bi layer around the SP2. We have found that for r0, the high positive potential energy (P.E) due to several overlap, therefore r0 is rejected. Among the non-overlapping configuration r1, r2 and r3. The r1 had least P.E. Hence, with r1 configuration we constructed pre-formed bilayer by using packmol.<sup>3,4</sup> taking CTAB 95 inner and 165 outer

**Table S3: Parameters used in the bilayer simulations**

$D_p$ (nm)	$N_{S1}$	$N_{S2}$	$N_{Br}$	$N_w$
2	95	165	260	46115
3	180	240	420	57032

$N_{Br}$ ,  $N_w$  are the number of  $Br^-$  and water molecules respectively.  $N_{S1}$  and  $N_{S2}$  are the number of CTAB molecules used in inner and outer layer of pre-formed bilayer respectively.

layer as shown in Fig.S12. We followed the similar procedure to form a bilayer by taking 180 CTAB with inner and 240 CTAB outer layer with SP3 AuNP as shown in Fig.S13 The number of water molecules, CTAB and counter ions are given in Table S3. The pre-formed bilayer of SP2 and SP3 are energy minimized as shown in Fig.S14 with same molecular dynamics simulation procedure discussed in materials and method in main manuscript.

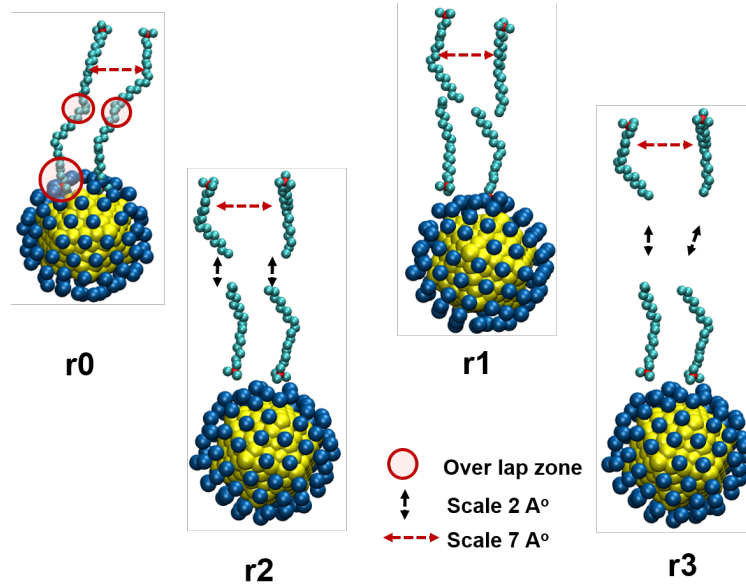


Figure S11: Four different initial configurations( r0, r1, r2 and r3 )SP2 95 Br coated with 2 CTAB.

Pre-formed bilayer of CTAB surfactants over SP3 surface (initial configuration) as shown in Fig.S15(a) Here  $Br^-$  freely distributed in bulk water for clarity both water molecules

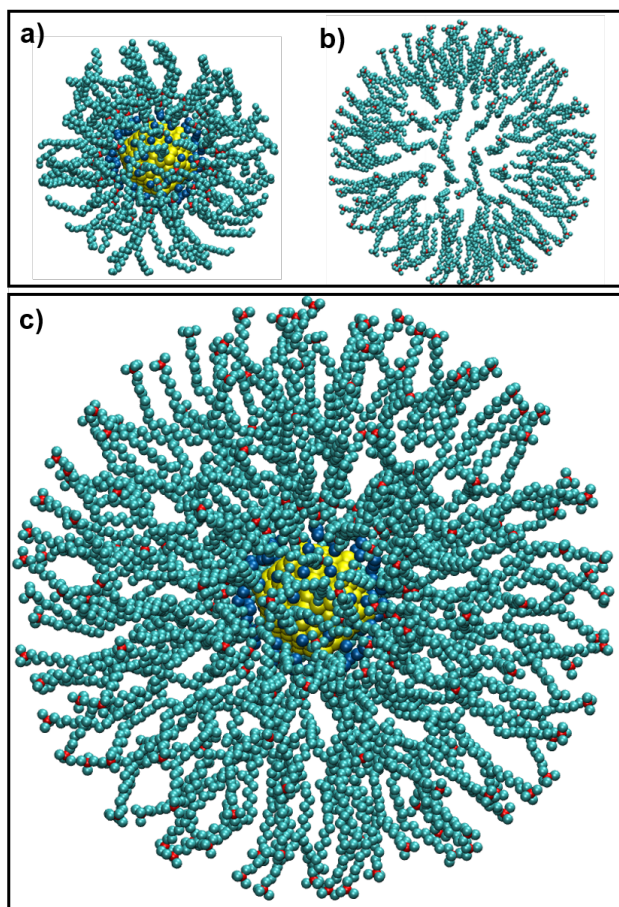


Figure S12: Bilayer construction of SP2. (a) Inner layer (b) Outer layer and (c) Bilayer.



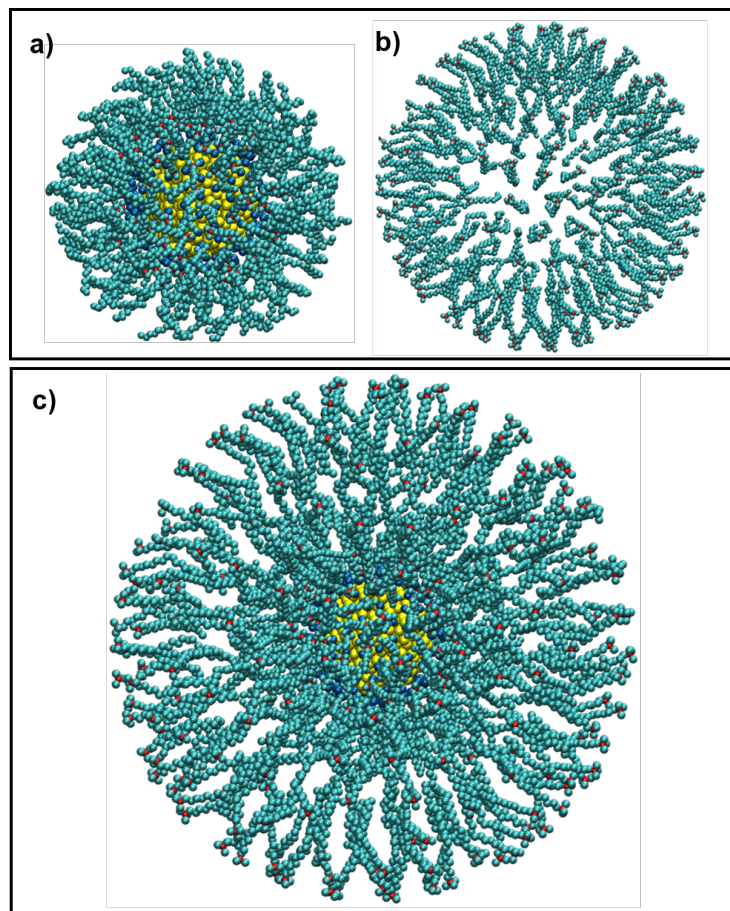


Figure S13: Bilayer construction of SP3. (a) Inner layer (b) Outer layer and (c) Bilayer.

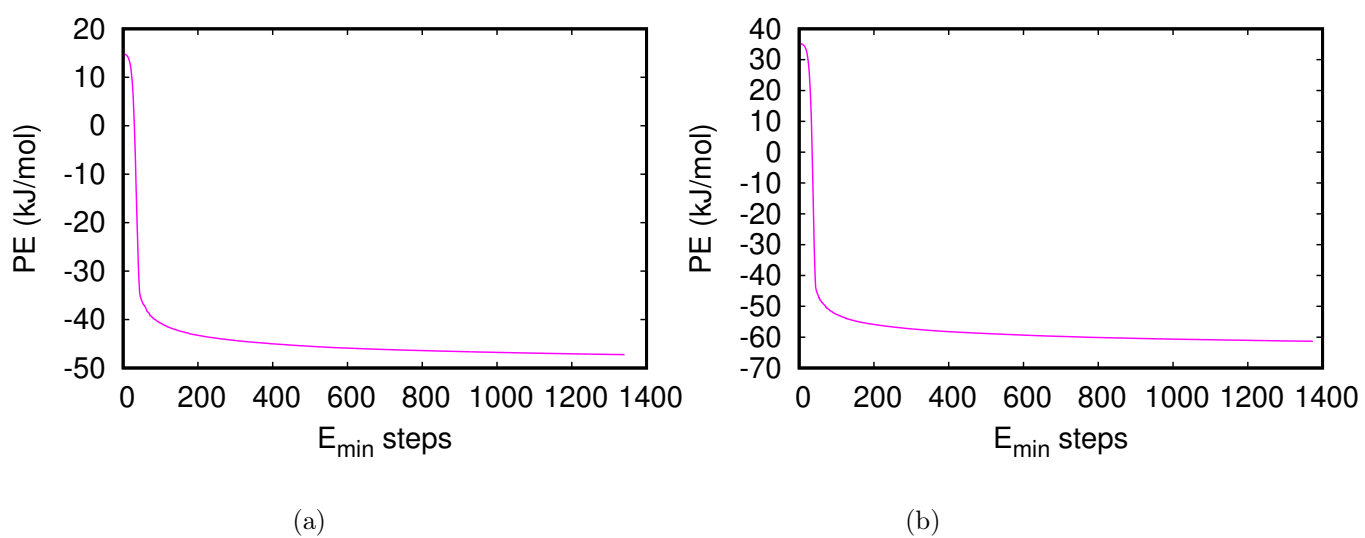


Figure S14: Energy minimization of pre-formed bilayer. (a) SP2 and (b) SP3.



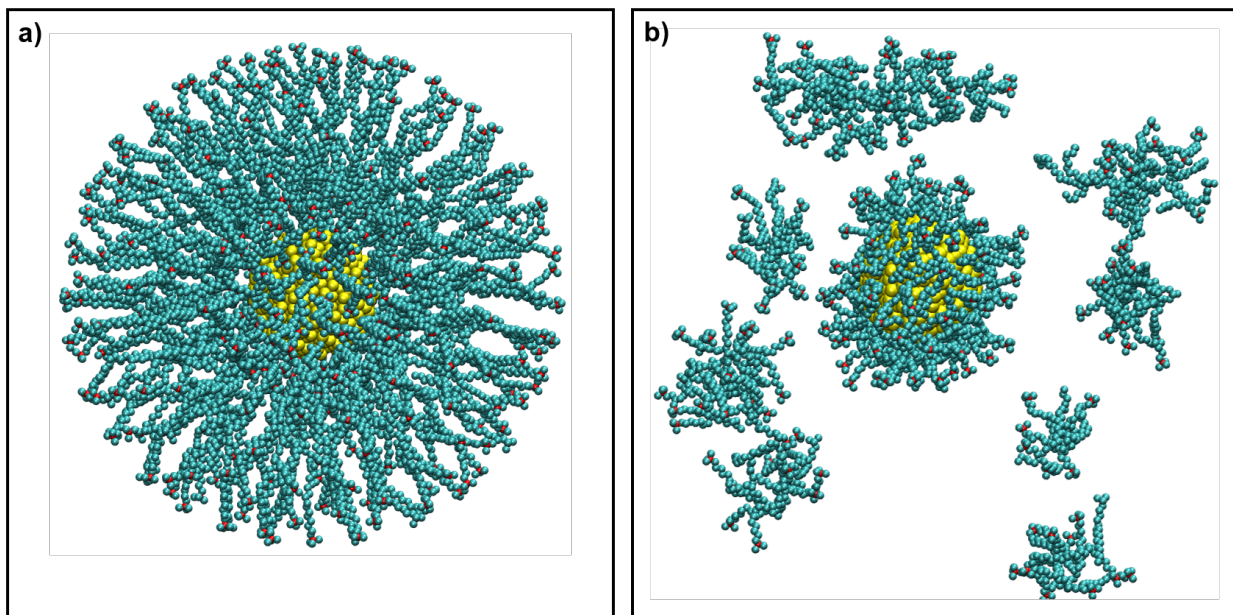


Figure S15: Pre-formed bilayer CTAB around SP3: (a) initial and (b) final configuration.

and free  $Br^-$  ions are not shown. After the energy minimization, 1 ns of NVT and NPT equilibration were done. Then, total 100 ns production run were done with same simulation procedure discussed in materials and method in main manuscript. The pre-formed bilayer structure was not stable and it forms monolayer over SP3 surface with tail wrapping around SP3 surface and head protruding out to bulk water. The final equilibrium configuration for SP3 is shown in Fig.S15(b).

Another set of pre-formed bilayer simulation for SP3 particle 180  $Br^-$  ions were immobilized on the surfaces. The corresponding initial configuration as shown in Fig.S16 (a). After the energy minimization, 1 ns of NVT and NPT equilibration were done. Then, total 100 ns production run were done with same simulation procedure discussed in materials and method in main manuscript. The final equilibrium configuration for SP3 are shown in Fig.S16(b). Here, also the pre-formed bilayer is not stable for SP3. However, we only observe islands of bicells around SP3. Similar to pre-formed bilayer with  $Br^-$  ions immobilized simulation for SP3. We, also done for SP2 with 95  $Br^-$  ions were immobilized on the surface and also observed similar islands of bicells around SP2. The corresponding initial and final configurations are shown in Fig.S17 (a) and (b).

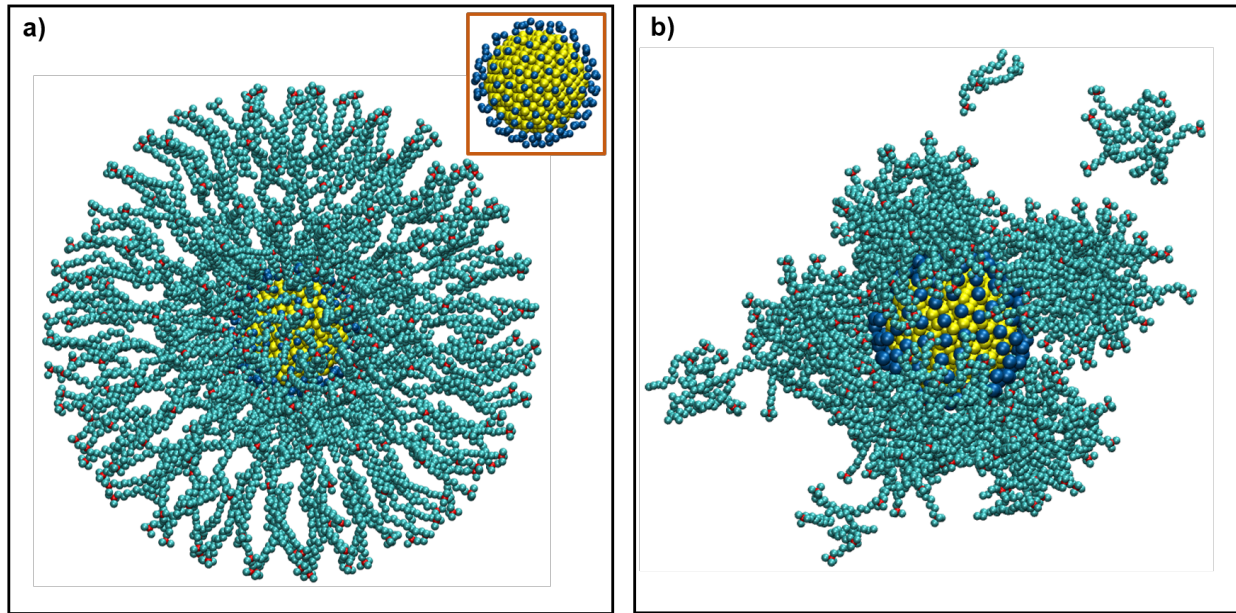


Figure S16: Bilayer CTAB with SP3: (a) initial configuration with inset highlighting  $Br^-$  immobilization and (b) final configuration.

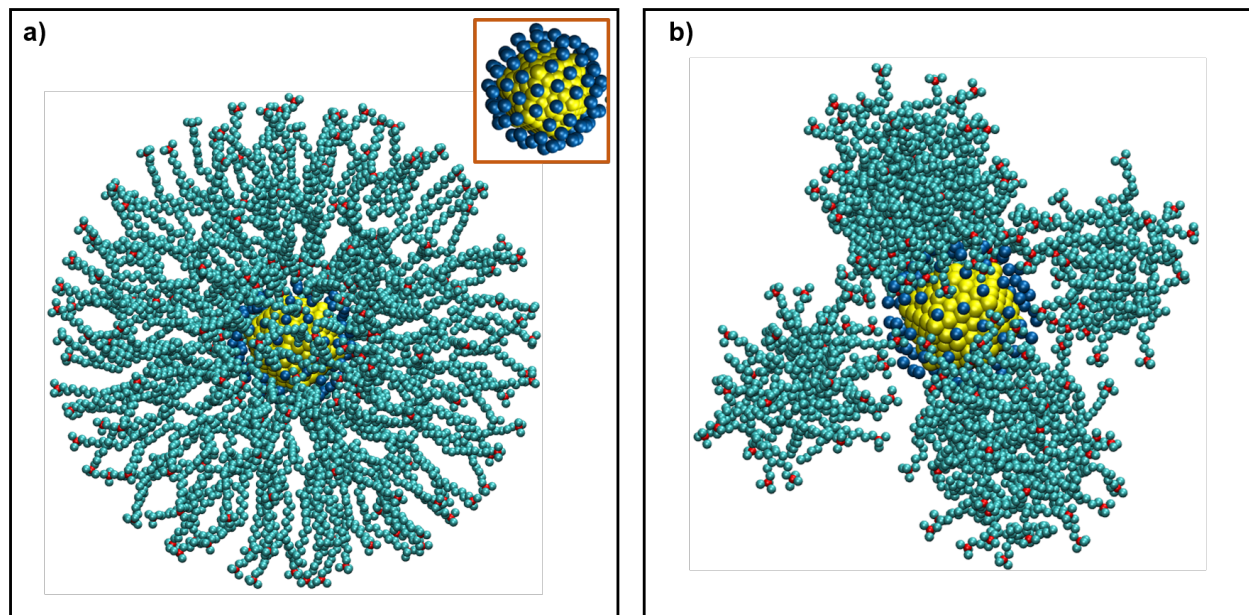


Figure S17: Bilayer CTAB with SP2: (a) initial configuration with inset highlighting  $Br^-$  immobilization and (b) final configuration.

## VI. Pre-formed bilayer on flat gold surface

We have considered two different works on adsorption of CTAB on planar gold surface by da Silva and Meneghetti<sup>5</sup> and Meena and Sulpizi<sup>6</sup> As shown below, we are able to reproduce

the results of these references provided the initial conditions are chosen as per their choice, whereas when we use random initial configurations the final equilibrium configuration of CTAB on flat gold surface is similar to that is found on spherical gold nanoparticles of size 1 - 3 nm. If sufficient number of  $Br^-$  ions are immobilized on the flat gold surface and an initial configuration of CTAB bilayer is used, we find that CTAB bilayer is stable, whereas for spherical nanoparticles of size 1 - 3 nm, bilayer was not stable even after immobilizing upto 50% of  $Br^-$  ions. Therefore we may conclude that if  $Br^-$  ions were to be near the gold surface due to polarization and/or quantum mechanical effects, bilayer may be formed on flat gold surface, whereas on tiny spherical seed particles such bilayer configuration is not stable. Therefore the curvature plays a role only when  $Br^-$  ions are immobilized. We now summarize the details of the simulations to support the above findings.

We have taken a  $4 \times 4 \text{ nm}^2$  flat gold slab (AuSL) of 250 plane. The AuSL was constructed from 1500 Au atoms, with a thickness (1.5 nm) greater than the LJ cutoff distance (1.4 nm). A total of 98 CTAB molecules (49 molecules on each layer) are used to construct a bilayer as shown in Fig. S18 on either side of the gold surface. A fraction of the  $Br^-$  ions, hereby referred to as Br-1, was placed closer to the gold surface. Rest of the  $Br^-$  ions were distributed in the bulk and they are denoted as Br-2 (see Table S4). The positions of Br-1 ions are fixed (immobilized), while Br-2 ions are allowed to move. The preparation of the system as above was motivated by the previous works (da Silva and Meneghetti,<sup>5</sup> and Meena and Sulpizi<sup>6</sup>) on CTAB adsorption on gold surface. The system was simulated for 200 ns simulation.

A visual comparison of the initial configurations between da Silva and Meneghetti,<sup>5</sup> and our simulations are shown in Fig. S18a and b, respectively. Even though the surfactant molecules were initially assembled as a bilayer, their stability was mainly dependent on the concentration of  $Br^-$  ions present near the gold surface (Br-1). When we immobilized 20  $Br^-$  ions each on either side of the gold surface, we observed that the initial bilayer structure transformed into cylindrical micelles as shown in Figure S19b. da Silva and Meneghetti<sup>5</sup>



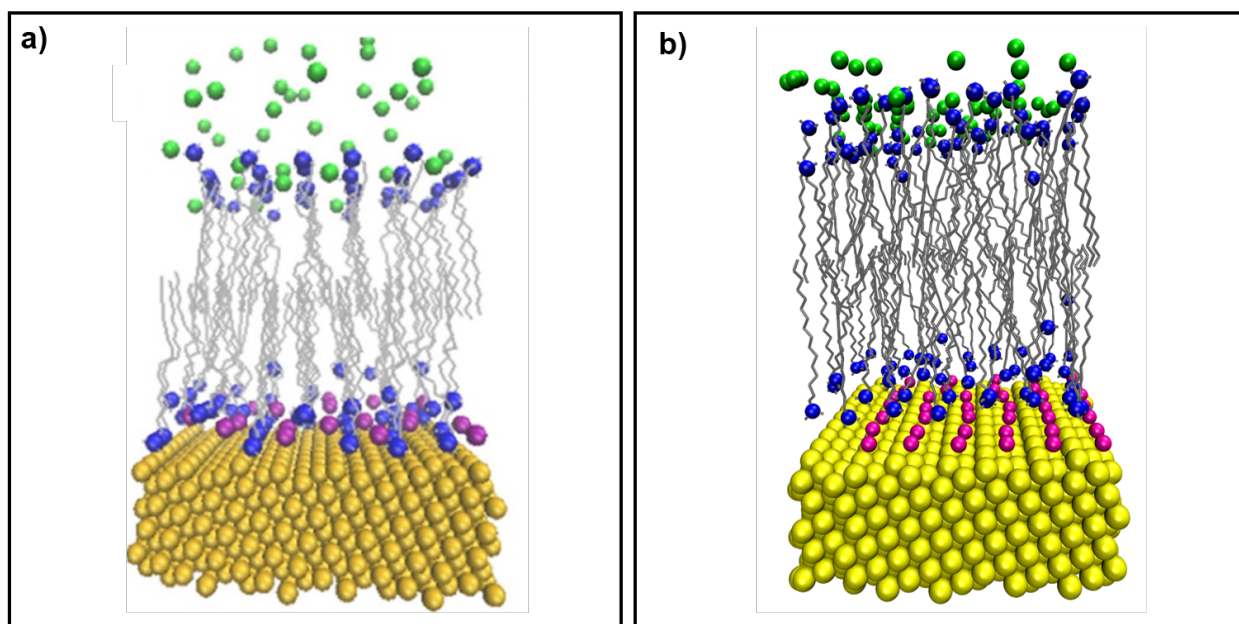


Figure S18: Initial CTAB bilayer configuration on planar gold  $\{250\}$  surface (a) da Silva and Meneghetti<sup>5</sup> (b) present work. Color coding: Gold atoms (yellow), nitrogen of the CTAB head group (blue), hydrophobic tail (gray), Br-1 (magenta), and Br-2 (green). Water molecules were omitted for clarity.

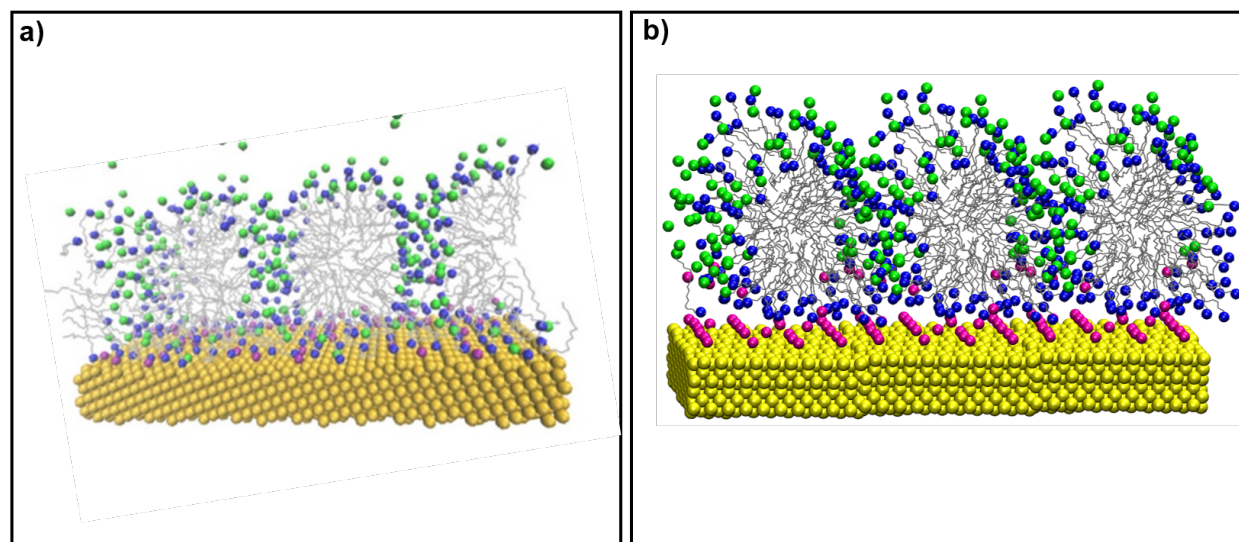


Figure S19: Equilibrium configurations of CTAB molecules on planar gold  $\{250\}$  surface shown with periodic images in the x-direction. Front view of the adsorbed CTAB molecules in the form of cylindrical micelles on the AuSL (a) da Silva and Meneghetti<sup>5</sup> (b) present work.

reported similar observations as shown in Figure S19a. We calculated the density profiles of various species normal to the gold surface in Figure S20b, which shows good agreement with that of da Silva and Meneghetti<sup>5</sup> (Fig. S20a). The density of non-polar tail groups (C20 atom) increases starting from a distance of 1 nm from the gold surface, due to which density of water drastically drops before reaching bulk density. A sharp peak in the C20 density indicates ordering by aliphatic tail groups and stabilizing micelles structure.

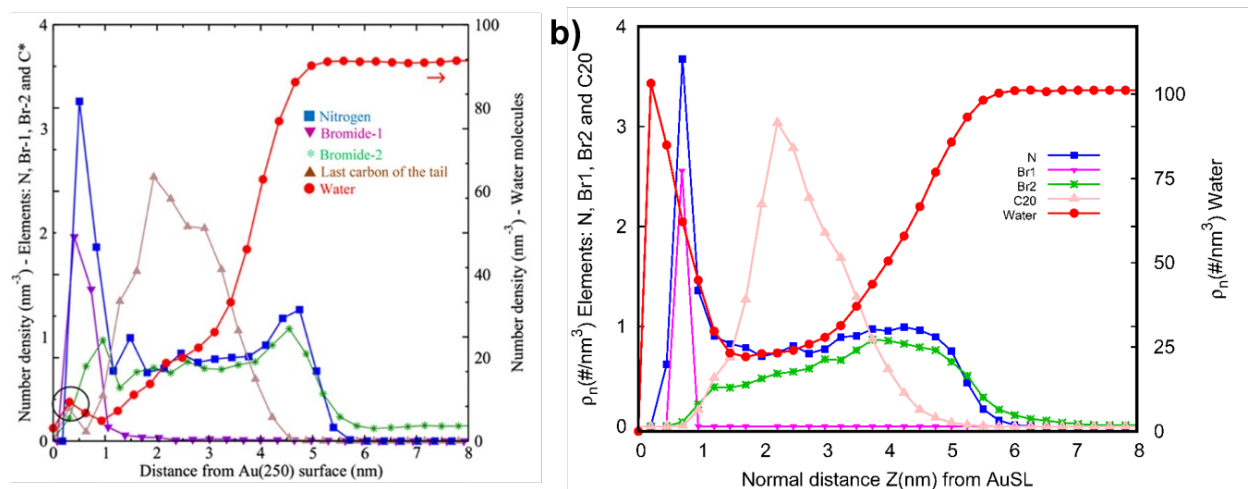


Figure S20: Number density of species normal to AuSL surface corresponding to Figure S19.

One notable difference is the presence of a water layer near the gold surface in our simulations, which was not observed in the simulations conducted by da Silva and Meneghetti.<sup>5</sup> As water channels exist between the adjacent micelles to facilitate diffusion of water from bulk to gold surface, it is unusual for the lack of water layer near the gold surface which contain polar nitrogen of the surfactant head group and  $Br^-$  counterions. The authors have not discussed any reason for this unusual result. However, for a similar system Meena and Sulpizi<sup>6</sup> have reported the presence of water layer near the gold surface. A comparison between our result and that of Meena and Sulpizi<sup>6</sup> is shown in Fig. S21. Existence of such water layer near gold surface was reported in one of our previous works, Kalipillai and Mani,<sup>7</sup> and by Shao and Hall.<sup>8</sup>

Next the simulation was repeated with 40 immobilized  $Br^-$  ions on both sides of the gold surface. A strong electrostatic attraction between the immobilized  $Br^-$  ions and the

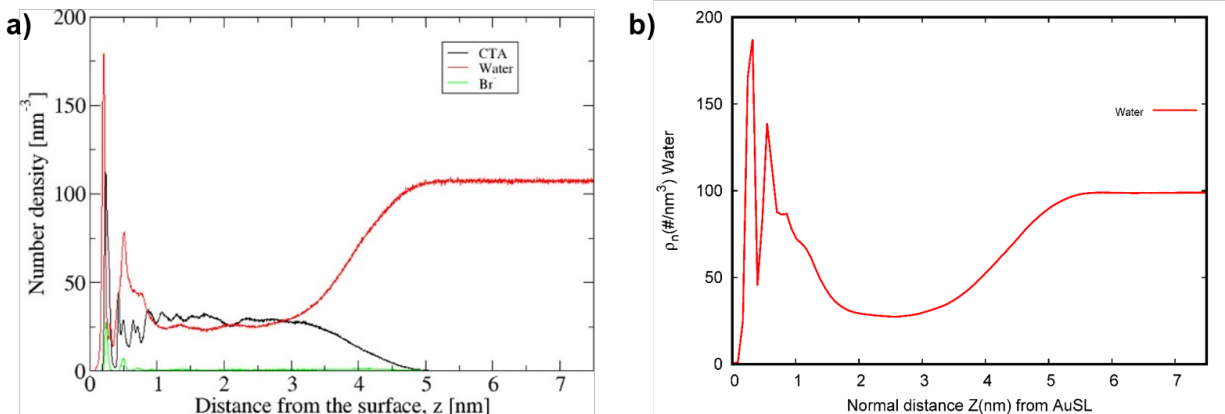


Figure S21: Number density profile of water normal to AuSL surface: (a) Meena and Sulpizi<sup>6</sup> and (b) present work.

head groups was previously attributed to the stabilization of the initial bilayer structure.<sup>5</sup> As discussed above, the water layer present near the gold surface acts as a dielectric medium and can screen electrostatic interactions. As a result, we notice a collapsed CTAB bilayer as shown in Figure S22b and for comparison the configuration reported by da Silva and Meneghetti<sup>5</sup> is also shown in Figure S22a. The density profile plot (Fig. S23) shows a similar densities near the gold surface for Br<sup>-</sup> (Br1) and head groups (N) between our simulations and that of da Silva and Meneghetti's work. Again, the presence of water layer in our system influences the distribution of Br2 ions.

Without immobilization of Br<sup>-</sup> ions and with random initial configuration of CTAB molecules, simulations show a different equilibrium configuration. As shown in Fig. S24, the tail of CTAB adsorb on gold surface with head group projecting towards bulk water. Excess CTAB molecules form spherical micelles in bulk water. This configuration is similar to what is seen on spherical particles (See Figure 3 in the revised manuscript).

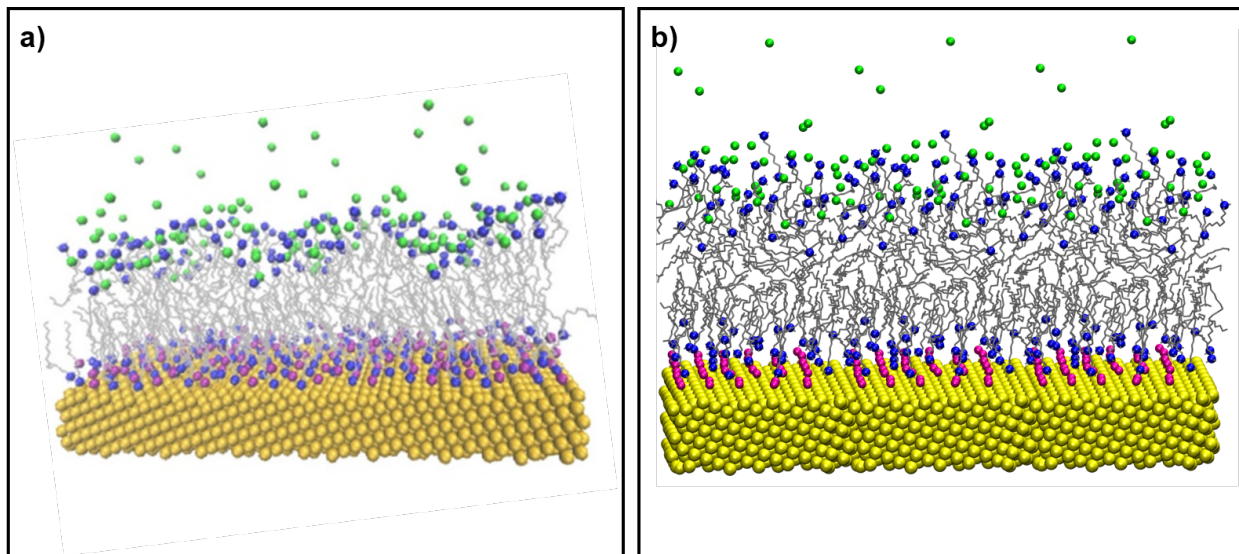


Figure S22: Equilibrium configurations of CTAB bilayer on planar AuSL surface shown periodic in x-direction:(a) da Silva and Meneghetti<sup>5</sup> (b) present work.

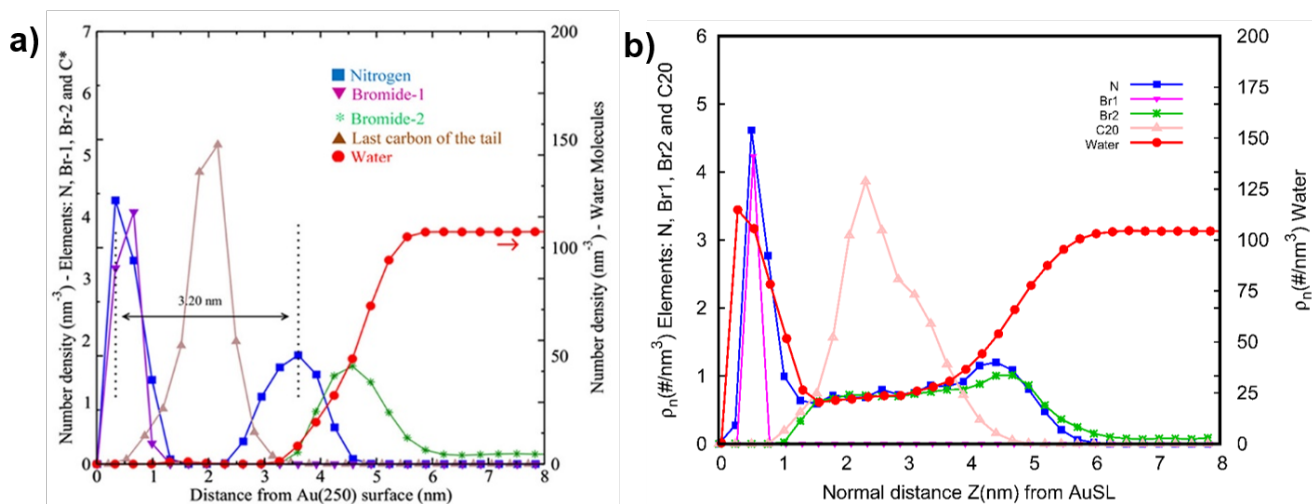


Figure S23: Number density of species normal to AuSL surface corresponding to Figure S22 : (a) da Silva and Meneghetti<sup>5</sup> and (b) present work.

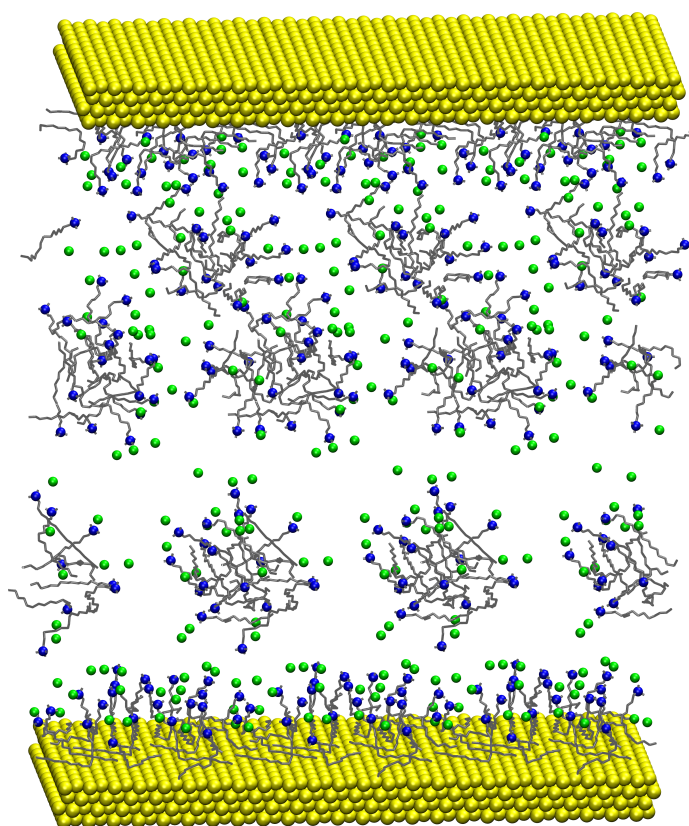


Figure S24: Equilibrium configuration of CTAB molecules on planar AuSL surface starting with random initial configuration, shown with periodic images in x-direction.



**Table S4: Parameters used in CTAB flat gold slab (AuSL)the simulations**

	CTAB bilayer-AuSL*	CTAB bilayer-AuSL**	CTAB random-AuSL
$N_s$	98+98	98+98	98
$N_{Br}$	40+158	80+118	98
$N_w$	5428	5428	6008

$N_s$ ,  $N_{Br}$ ,  $N_w$  are the number of CTAB,  $Br^-$  and water, respectively. \* 20% Br-1 is fixed, \*\*40% Br-1 is fixed on AuSL surface.

## References

- (1) Kumari, R.; Kumar, R.; Consortium, O. S. D. D.; Lynn, A. g\_mmpbsa A GROMACS tool for high-throughput MM-PBSA calculations. *Journal of chemical information and modeling* **2014**, *54*, 1951–1962.
- (2) Lide, D. R., et al. CRC handbook of chemistry and physics, internet version 2005. 2005.
- (3) Martínez, J. M.; Martínez, L. Packing optimization for automated generation of complex system’s initial configurations for molecular dynamics and docking. *Journal of computational chemistry* **2003**, *24*, 819–825.
- (4) Martínez, L.; Andrade, R.; Birgin, E. G.; Martínez, J. M. PACKMOL: a package for building initial configurations for molecular dynamics simulations. *Journal of computational chemistry* **2009**, *30*, 2157–2164.
- (5) da Silva, J. A.; Meneghetti, M. R. New aspects of the gold nanorod formation mechanism via seed-mediated methods revealed by molecular dynamics simulations. *Langmuir* **2018**, *34*, 366–375.
- (6) Meena, S. K.; Sulpizi, M. Understanding the microscopic origin of gold nanoparticle

- anisotropic growth from molecular dynamics simulations. *Langmuir* **2013**, *29*, 14954–14961.
- (7) Kalipillai, P.; Mani, E. Adsorption of the amyloid  $\beta$ 40 monomer on charged gold nanoparticles and slabs: a molecular dynamics study. *Physical Chemistry Chemical Physics* **2021**, *23*, 18618–18627.
- (8) Shao, Q.; Hall, C. K. Binding preferences of amino acids for gold nanoparticles: a molecular simulation study. *Langmuir* **2016**, *32*, 7888–7896.